Spin relaxation through lateral spin transport in heavily doped *n*-type silicon

M. Ishikawa,[1,2] T. Oka,[1] Y. Fujita,[1] H. Sugiyama,[2] Y. Saito,[2] and K. Hamaya[1,3,*]

[1]*Department of Systems Innovation, Graduate School of Engineering Science, Osaka University, 1-3 Machikaneyama, Toyonaka 560-8531, Japan*

[2]*Corporate & Research Development Center, Toshiba Corporation, 1 Komukai-Toshiba-cho, Kawasaki, Kanagawa 212-8582, Japan*

[3]*Center for Spintronics Research Network, Graduate School of Engineering Science, Osaka University, 1-3 Machikaneyama, Toyonaka 560-8531, Japan*

(Received 4 November 2016; revised manuscript received 27 January 2017; published 3 March 2017)

We experimentally study temperature-dependent spin relaxation including lateral spin diffusion in heavily doped *n*-type silicon (n^+-Si) layers by measuring nonlocal magnetoresistance in small-sized CoFe/MgO/Si lateral spin-valve (LSV) devices. Even at room temperature, we observe large spin signals, 50-fold the magnitude of those in previous works on n^+-Si. By measuring spin signals in LSVs with various center-to-center distances between contacts, we reliably evaluate the temperature-dependent spin diffusion length (λ_{Si}) and spin lifetime (τ_{Si}). We find that the temperature dependence of τ_{Si} is affected by that of the diffusion constant in the n^+-Si layers, meaning that it is important to understand the temperature dependence of the channel mobility. A possible origin of the temperature dependence of τ_{Si} is discussed in terms of the recent theories by Dery and co-workers.

DOI: 10.1103/PhysRevB.95.115302

I. INTRODUCTION

Studies of spin transport in semiconductors such as GaAs [1–5], Si [6–10], and Ge [11–14] have been reported for achieving semiconductor spintronics devices [15,16]. Si, in particular, has been expected to transport long-lived spin information in semiconductor devices because of long spin diffusion length and spin lifetime due to the weak spin-orbit coupling and lattice inversion symmetry in the crystal structure [17–20]. So far, 350-μm-long spin transport has been observed in undoped single-crystal Si by using ballistic hot-electron spin injection [10]. Recently, the influence of electron-phonon interactions [17–20] and donor impurities [21,22] on the spin relaxation in doped Si has been discussed in detail.

Recent progress in spin injection and detection techniques in heavily doped *n*-Si (n^+-Si) layers has enabled observation of room-temperature spin transport in lateral spin-valve devices [8,9]. Previously, Suzuki *et al.* reported that the spin diffusion length (λ_{Si}) of n^+-Si at room temperature is estimated to be $\sim$0.6 μm from Hanle-effect curves obtained by four-terminal nonlocal (NL) magnetoresistance measurements [8]. Although they also showed the temperature dependence of λ_{Si} and the spin lifetime (τ_{Si}) in n^+-Si by fitting Hanle-effect signals, the mechanism of the temperature dependence has remained an open question.

A recent theory by Song *et al.* indicated that multivalley semiconductors such as Si exhibit a donor-driven spin relaxation mechanism due to the central-cell potential of the doped impurities [21]. This theory suggests that when the above mechanism is dominant, the spin lifetime is temperature independent and depends only on the donor concentration in heavily doped semiconductors ($\epsilon_{\mathbf{k}} \approx k_B T$), where $\epsilon_{\mathbf{k}}$ is the energy of the conduction electron above the band edge and k_B is Boltzmann's constant. However, an experiment by Suzuki *et al.* showed reduction in τ_{Si} from 10 ns to 1.3 ns with elevating temperature even in n^+-Si [8]. Thus, the spin relaxation mechanism due to electron-phonon interaction needs to be discussed even for n^+-Si [17–20]. From the viewpoint of spin relaxation in n^+-Si, since the temperature dependence of τ_{Si} remains unclear, the spin transport and spin relaxation in n^+-Si need to be examined in further detail.

In this article, we study four-terminal NL spin transport [23–25] at various temperatures in lateral spin-valve devices with a small size (0.305 μm^2) cross section in the n^+-Si layer. Even at room temperature, we observe large spin signals, 50-fold of the magnitude observed in previous works on n^+-Si [8,9]. The temperature dependences of λ_{Si} and τ_{Si} are accurately estimated from evaluating the center-to-center distance dependence of the spin signals. We find that the temperature dependence of τ_{Si} is affected by that of the diffusion constant (D) in n^+-Si layers. This means that it is important for understanding the spin relaxation in n^+-Si to consider the channel mobility (μ). A possible origin of the temperature dependence of τ_{Si} is discussed in terms of the recent theories by Dery and co-workers [17,18,21].

II. SAMPLES AND MEASUREMENTS

MgO films ($\sim$1.1 nm) were deposited to act as a tunnel barrier at 200 °C on a phosphorus-doped ($n \sim 1.6\times 10^{19}$ cm^{-3}) (100)-textured SOI (61 nm) layer by electron-beam evaporation. A CoFe layer (15 nm) and Ru cap layer (7 nm) were then sputtered on top under a base pressure better than 5.0×10^{-7} Pa [9,26]. Conventional processes with electron-beam lithography, Ar^+ ion milling, and reactive-ion etching were used to fabricate lateral spin valves (LSVs). Figure 1(a) shows a top-view optical micrograph of a fabricated LSV. The Ru/CoFe/MgO contacts were patterned into dimensions of $2.0 \times 5.0\,\mu$m^2 and $0.5 \times 5.0\,\mu$m^2, respectively, and the channel width was 7.0 μm. Finally, ohmic pads consisting of Au/Ti were formed for all contacts. The cross-sectional area of the n^+-Si layer was 0.305 μm^2. The center-to-center distances (d) between CoFe/MgO contacts are designed to be

*hamaya@ee.es.osaka-u.ac.jp

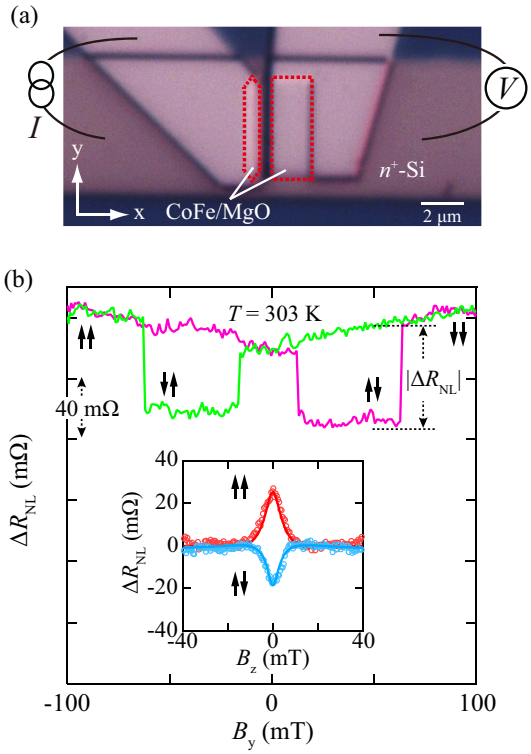

FIG. 1. (a) Optical micrograph of a fabricated n^+-Si–based LSV. (b) Nonlocal magnetoresistance curve at 303 K. The inset shows nonlocal four-terminal Hanle-effect curves for the parallel and antiparallel magnetization configurations at 303 K. The solid curves are the results of fitting to Eq. (2) in Ref. [24].

1.55, 1.65, 1.75, 2.25, 3.25, and 3.75 μm. By using the NL terminal configuration [see Fig. 1(a)], electrical measurements were carried out using a conventional dc-bias technique at various temperatures. External magnetic fields, B_y and B_z, were applied to the directions along the in-plane and out-of-plane, respectively, for the LSVs.

III. RESULTS AND DISCUSSION

A. Spin diffusion length in n^+-Si

Figure 1(b) shows a four-terminal NL magnetoresistance signal ($\Delta R_{NL} = \Delta V_{NL}/I$) at a bias current of -1.0 mA at 303 K, where d was 1.75 μm. We can clearly see a spin-valve-like signal at room temperature. We also observed a broad change in the background resistance, indicating that the magnetic configuration of the parallel state at around zero field was unstable in the fabricated CoFe/MgO/SOI devices. Although the origin of this behavior is under discussion, NL signals can also change steeply with the maximum ΔR_{NL} value when the magnetization configuration between the spin injector and detector is switched from antiparallel to parallel at a higher field (B_y). Thus, we hereafter define $|\Delta R_{NL}|$ as a steep change in the value of ΔR_{NL} at $B_y \approx 60$ mT, as shown in Fig. 1(b). Four-terminal NL Hanle signals for the same device at 303 K are also shown in the inset of Fig. 1(b), which shows evidence for spin injection, manipulation, and detection in n^+-Si. It should be noted that $|\Delta R_{NL}|$ in Fig. 1(b) reaches 65 mΩ, which is approximately 50-fold the value given in

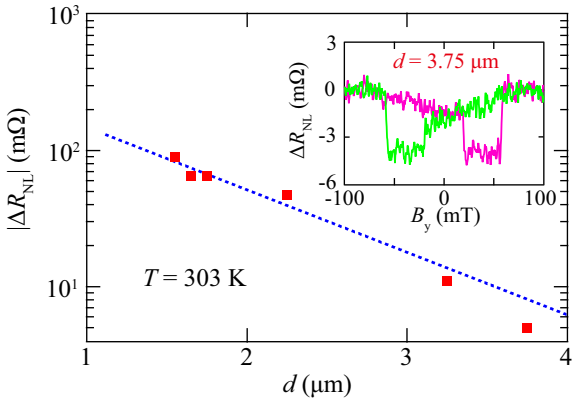

FIG. 2. d dependence of $|\Delta R_{NL}|$ at 303 K. The dashed line shows the results of fitting to Eq. (1). The inset is the NL magnetoresistance curve at 303 K for a device with $d = 3.75$ μm.

Ref. [8]. In general, $|\Delta R_{NL}|$ can be expressed by the following equation [26–29]:

$$|\Delta R_{NL}| = \frac{4|P_{inj}||P_{det}|r_{Si}r_b^2 \exp\left(-\frac{d}{\lambda_{Si}}\right)}{S_N\left\{(2r_b + r_{Si})^2 - r_{Si}^2 \exp\left(-\frac{2d}{\lambda_{Si}}\right)\right\}}, \quad (1)$$

where P_{inj} and P_{det} are spin polarizations of the electrons in Si created by the spin injector and detector, respectively, and r_b and r_{Si} are the resistances of the CoFe/MgO interface and the n^+-Si layer. S_N is the cross-sectional area (0.305 μm^2) of the n^+-Si layer. In previous works [8,9,26], the S_N values were relatively large (1.68 μm$^2 \leqslant S_N \leqslant$ 5.0 μm^2), compared to this work. Since we utilized a small cross section in the n^+-Si layer as a spin transport channel [27,30–33], we detected quite large spin signals in order to precisely estimate λ_{Si} and τ_{Si} from electrically measuring spin transport at various temperatures. Although Tahara *et al.* recently reported large spin signals of several Ω in Si at room temperature, the used spin transport layer is a nondegenerate n-Si, leading to large spin accumulation [34]. Since this study focuses on the spin relaxation mechanism in n^+-Si (degenerate n-Si), the enhancement in $|\Delta R_{NL}|$ due to the small cross section in the spin transport layer is useful.

Next, we examine the dependence of $|\Delta R_{NL}|$ on d at 303 K in Fig. 2. Since $|\Delta R_{NL}|$ is much larger than in previous works, we can observe spin signals for the LSV with $d = 3.75$ μm (see inset of Fig. 2) and an exponential decay of $|\Delta R_{NL}|$ with an increase in d is seen. Using Eq. (1), we extract the room-temperature λ_{Si} of ∼0.95 μm. Although this value is slightly larger than λ_{Si}(≈0.6 μm) in Ref. [8], we can recognize that our data is more reliable because of the large spin signals from using small-sized devices. We also extracted λ_{Si} ($=\sqrt{D\tau_{Si}}$) from the fitting of the NL Hanle-effect curves based on the one-dimensional spin drift diffusion model [1,24]. The solid curves in the inset of Fig. 1(b) show representative results of the fitting to Eq. (2) of Ref. [24]. As a result, the τ_{Si} and D values at 303 K for the n^+-Si layer were estimated to be 0.7 ns and 20 cm^2/s, respectively, leading to a λ_{Si} of 1.2 μm at 303 K, also consistent with the above framework. Since the analytical data from these electrical Hanle-effect measurements have already been reported in Ref. [8], we will focus on the extraction from Eq. (1) by using the dependence of $|\Delta R_{NL}|$ on d [35].

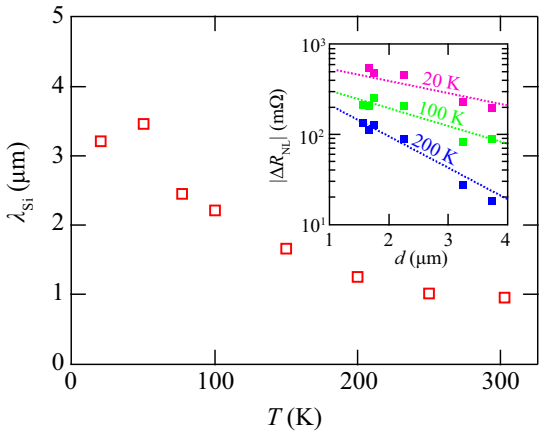

FIG. 3. Temperature dependence of λ_{Si} estimated by d dependences of NL spin signals at various temperatures, as shown in the inset.

For all the LSVs, we measured the dependence of $|\Delta R_{NL}|$ on d at various temperatures (see inset of Fig. 3), and then λ_{Si} as a function of temperature was obtained in Fig. 3. At 20 K, the λ_{Si} value is enhanced up to ~ 3.2 μm. These features are similar to previous works [8,36]. We speculate that this similarity is due to the nature of spin-related scattering in the n^+-Si layer ($n \approx 10^{19}$ cm^{-3}). We discuss the spin relaxation phenomena in the n^+-Si layer in terms of this nature.

B. Spin lifetime in n^+-Si

For heavily doped semiconductors, the D value of spins should be calculated from Eq. (4) in Ref. [37]. Since the D values are strongly related to the μ value, we have to obtain μ in the n^+-Si layer used here. Using the Hall-bar device of the n^+-Si layer (100×100 μm^2), we measured the temperature dependence of n and resistivity (ρ_{Si}), leading to the temperature dependence of μ, as shown in the inset of Fig. 4(b). Because a large change in n was not observed as the temperature changed, μ was slightly reduced with increasing temperature because of the metallic ρ_{Si} behavior. From the μ values and Eq. (4) in Ref. [37], the D values are calculated as a function of temperature as shown in Fig. 4(a). For the n^+-Si layer used here, we can regard the characteristics of D as consequences of μ in the spin transport layer.

By using the relation $\lambda_{Si} = \sqrt{D\tau_{Si}}$ and the results in Figs. 3 and 4(a), the temperature dependence of τ_{Si} is given as solid symbols in Fig. 4(b). It should be noted that τ_{Si} is $\sim$2.1 ns at 303 K and is enhanced up to $\sim$16.4 ns with decreasing temperature, implying that τ_{Si} depends on external temperature. Interestingly, the temperature dependence of τ_{Si} in this work is consistent with that in Ref. [8]. From these calculations, this study elucidated that the temperature dependence of τ_{Si} is correlated with that of D. Since this work is based on the pure spin current transport toward lateral dimensions in the n^+-Si layer, we should consider the influence of the intrinsic nature in the n^+-Si layer on the spin relaxation under the lateral spin transport. Notably, we find that the behavior of the temperature dependence of τ_{Si} in Fig. 4(b) is similar to that of D in Fig. 4(a). For the n^+-Si layer in the range from 20 to 303 K, the D value arises from the μ value in the transport layer on the basis of Eq. (4) in Ref. [37]. Namely, we can infer that μ in the n^+-Si layer affects τ_{Si}.

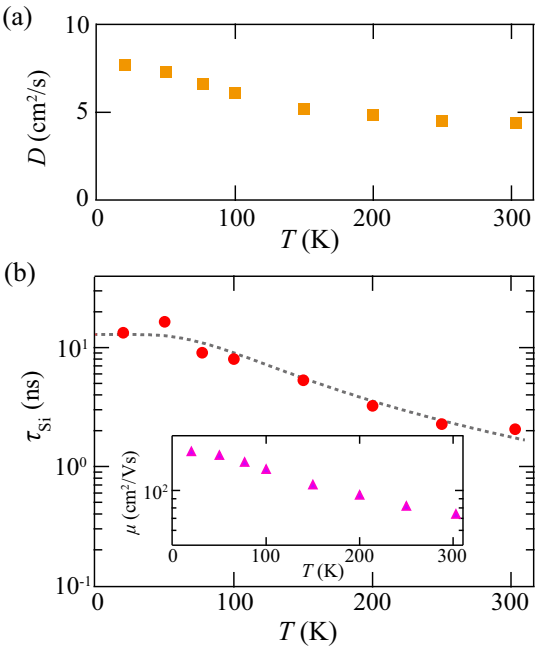

FIG. 4. (a) Temperature dependence of D, estimated from Eq. (4) in Ref. [37]. (b) Temperature dependence of τ_{Si} in the n^+-Si layer used, together with the theoretical fitting curve (gray dashed curve) is based on Eqs. (2)–(5). The inset shows the temperature dependence of μ in the n^+-Si layer used.

C. Comparison of experiment and theory

In general, the spin relaxation in undoped Si is discussed in terms of the Elliott-Yafet mechanism including the conduction-band valley anisotropy [6,10,17–19]. Recently, Dery and co-workers reexamined the Elliott-Yafet mechanism in multivalley semiconductor systems and predicted the detailed spin relaxation due to electron-phonon interactions in the multivalley conduction band in Si [17,18]. Since the temperature dependence of τ_{Si} in n^+-Si is related to that of D, as described in Fig. 4, we have to regard the temperature-dependent μ shown in the inset of Fig. 4 as an important factor for understanding the spin relaxation mechanism. In short, since the $\mu - T$ curve indicates the presence of phonon-induced carrier scattering, we need to consider the spin relaxation due to the electron-phonon interactions in n^+-Si. In addition, Dery and co-workers also suggested donor-driven spin relaxation for doped Si [21]. The conduction band dominated by the multivalley nature causes short-range spin-flip scattering due to the central-cell potential of impurities doped. The following discusses the temperature dependence of τ_{Si} in terms of these theories [17,18,21].

According to Matthiessen's rule for Si, the following spin scattering rate ($\frac{1}{\tau_{Si}}$) needs to be considered:

$$\frac{1}{\tau_{Si}} = \frac{1}{\tau_{imp}} + \frac{1}{\tau_{inter}} + \frac{1}{\tau_{intra}}, \quad (2)$$

where $\tau_{\rm imp}$, $\tau_{\rm inter}$, and $\tau_{\rm intra}$ are spin lifetimes due to impurity-induced, phonon-induced intervalley, and phonon-induced intravalley spin-flip scatterings, respectively [17,18,21]. Both $\tau_{\rm imp}$ and $\tau_{\rm inter}$ consist of so-called g and f processes (τ_g and τ_f) which arise from electron scattering between opposite valleys and valleys derived from perpendicular crystal axes, respectively [17,18,21,38]. Since it is well known that the contribution of the $\frac{1}{\tau_{\rm intra}}$ term is much weaker than other terms [17,18,21,38], we ignore this term from now on [39].

For $\tau_{\rm imp}$, since the g process is much smaller than the f process, the theory clarifies that the spin relaxation rate of a conduction electron with $\epsilon_{\mathbf{k}}$ above the band edge can be expressed as the following equation [21]:

$$\frac{1}{\tau_{\rm imp}} = \frac{4\pi N_{\rm d} m_{\rm e} a_B^6}{27\hbar^4}\sqrt{2m_{\rm e}\epsilon_{\mathbf{k}}}(6|\eta|^2+1)\Delta_{\rm so}^2, \tag{3}$$

where $N_{\rm d}$ is the donor concentration, $m_{\rm e}$ (=0.32 m_0) is the electron effective mass in Si, $a_{\rm B} \approx 2$ nm is the electron Bohr radius in Si, $\Delta_{\rm so} \approx 0.03$ meV is the spin-orbit-coupling–induced splitting of the triplet degenerate states in the conduction-band valley for Si:P [40,41], and $\eta = |\Delta'_{\rm so}/\Delta_{\rm so}| \approx 2$ is an empirical value [21], where $\Delta'_{\rm so}$ is the $1s(E)$ donor state splitting-related parameter and $\Delta_{\rm so}$ is the $1s(T_2)$ donor state splitting. For the case of $\epsilon_{\mathbf{k}} \approx k_{\rm B}T$, the scattering rate ($\frac{1}{\tau_{\rm imp}}$) in Eq. (3) exhibits $\sqrt{T}$ behavior. However, for the case of $\epsilon_{\mathbf{k}} \gtrsim k_{\rm B}T$, the scattering rate depends only on $N_{\rm d}$ because of $\epsilon_{\mathbf{k}} \approx \epsilon_{\rm F}$, where $\sqrt{2m_{\rm e}\epsilon_{\rm F}}/\hbar \approx (3\pi^2 N_{\rm d})^{1/3}$. When we use the n^+-Si layer ($n \approx 10^{19}$ cm^{-3}) and assume that the doped impurities (P) are completely ionized in the Si channel layer, we need to consider the latter case with $N_{\rm d} \approx n$.

For $\tau_{\rm inter}$, the g process can be expressed as follows [17,18]:

$$\frac{1}{\tau_g} = \frac{32}{9}\frac{m_t}{m_{cv}}\left(\frac{\Delta_X}{\Delta_C}\right)^2\left(\frac{2m_d}{\pi}\right)^{\frac{3}{2}}\frac{\sqrt{\Omega_g}D_g^2}{\hbar^2\varrho E_{g,X}}\frac{g(y)}{\exp(y)-1}. \tag{4}$$

$m_t = \frac{m_0 m_{cv}}{m_0+m_{cv}}$ is the transverse electron mass, where $m_{cv} = \hbar^2 E_{g,X}/2P^2$, $E_{g,X} \approx 4.3$ eV is the energy gap at the X point, $P \approx 9$ eV·Å is the mass anisotropy [42], $\Delta_X \approx 3.5$ meV is the spin-orbit-coupling–related parameter, $\Delta_C \approx 0.5$ eV denotes the energy spacing between the conduction bands at the conduction-band minimum position [17], $m_d = (m_0 m_t^2)^{1/3}$ is the effective electron mass, $\Omega_g \approx 21$ meV is the longitudinal acoustic phonon energy, $D_g \approx 4$ eV/Å is the intraband dilation and uniaxial deformation potential related constant [17,18,43], $y = \Omega_g/k_{\rm B}T$, and $g(y)$ is associated with the modified Bessel function of the second kind via $g(y) = \frac{\sqrt{y}}{2}\exp(\frac{y}{2})K_2(\frac{y}{2}) \approx 1 + 5y^{-\frac{3}{2}}$. On the other hand, the f process can be described by the following equation:

$$\frac{1}{\tau_f} = \frac{16}{3}\left(\frac{\Delta'_X}{E_{g,X}}\right)^2\left(\frac{2m_d}{\pi}\right)^{\frac{3}{2}}\sum_{i=1,3}\frac{A_i D_i^2}{\hbar^2\varrho\sqrt{\Omega_{f,i}}}\frac{f(y_i)}{\exp(y_i)-1}, \tag{5}$$

where $\Delta'_X \approx 5$ meV is the spin-orbit-coupling–related parameter, A_i ($A_1 = 2$ and $A_3 = 1$) is the spin-orientation-related parameter [17,18], D_i (D_1 and D_3) is a scattering constant associated with a phonon mode of Σ_i symmetry, $\Omega_{f,i}$ ($\Omega_{f,1} \approx 47$ meV and $\Omega_{f,3} \approx 23$ meV) is the Σ_i phonon energy [17,18], and $f(y) = \sqrt{y}\exp(y/2)K_{-1}(y/2)$ is associated with the modified Bessel function of the second kind.

By considering Eqs. (2)–(5), we fit the experimental data, as shown in Fig. 4(b) (see gray dashed curve), using $\tau_{\rm imp}$ and D_i (D_1 and D_3) in Eq. (5) as fitting parameters. Consequently, the best fit curve can be obtained by using the parameters of $\tau_{\rm imp} = 12.9$ ns, $D_1 = 1.95 \times 10^{-7}$ eV/Å, and $D_3 = 24.5$ eV/Å. When we calculated the $\tau_{\rm imp}$ value only from Eq. (3), we obtained $\tau_{\rm imp} \approx 11$ ns, nearly consistent with the best fit parameter. In addition, the obtained large difference in D_i between D_1 and D_3 likely implies that there is a large scattering difference based on the crystal orientation relative to the direction of injected spins. The detailed features will be discussed in future work. From these considerations, we can explain the temperature-dependent $\tau_{\rm Si}$ as a consequence of impurity- and phonon-induced spin scatterings by using the theories by Dery and co-workers [17,18,21].

In the field of semiconductor spintronics, the spin relaxation mechanism in semiconductors has been discussed for ten or more years. For n-GaAs channels, very long spin diffusion lengths ($\lambda_{\rm GaAs}$) of several micrometers at low temperatures have been reported every time and clear electrical spin signals have been observed even in very large LSVs, despite the presence of many spin relaxation mechanisms [1–5]. When one focuses on the μ value, the values for the moderately doped GaAs channels ($\mu \sim$ several hundreds of cm^2/V·s) are 1 order of magnitude larger than those ($\mu \sim$ several tens of cm^2/V·s) for the n^+-Si channel [44,45]. By considering Fig. 4, we can recognize that the temperature-dependent $\tau_{\rm Si}$ in n^+-Si layers originates from the weak temperature-dependent D and μ. In short, despite the weak spin-orbit coupling and lattice inversion symmetry in Si, the relatively low μ is the critical disadvantage for the lateral spin diffusion in n^+-Si channels, even at low temperatures. Therefore, when the spin relaxation with the diffusive spin transport in semiconductor channels is discussed, the influence of the D value associated with the μ value should be taken into account. In the field of quantum information technologies, on the other hand, Si has shown powerful advantages for the long coherence time and high fidelity when few-electron spins are treated on the quantum-dot platform [46–48]. In these ultimate devices, even the field induced by nuclear spins can affect the spin lifetime. Therefore, if the spin relaxation phenomena in semiconductor materials are discussed, one should also consider the situation of the related spins in the device structures. Since this study has clarified the origin of the temperature dependence of $\tau_{\rm Si}$, the device structures for realizing high-performance Si-based spintronic applications can be reconsidered.

IV. CONCLUSION

We have studied four-terminal NL spin transport at various temperatures in LSV devices with a small size cross section (0.305 μm^2) in the n^+-Si layer. We observed large spin signals, even at room temperature, 50-fold the magnitude observed

in previous works [8,9]. From evaluating the center-to-center distance dependence of the spin signals, we can accurately estimate the temperature dependences of λ_{Si} and τ_{Si}. We found that the temperature dependence of τ_{Si} is affected by that of D in the n^+-Si layer. We also clarified that the temperature dependence of τ_{Si} can be interpreted in terms of recent theories based on impurity- and phonon-induced spin relaxation mechanisms in doped multivalley semiconductors. We conclude that the temperature-dependent τ_{Si} in n^+-Si layers originates from the temperature-dependent μ and D in the n^+-Si layers.

ACKNOWLEDGMENTS

This work was partly supported by the ImPACT Program of the Council for Science, Technology and Innovation (Cabinet Office, Government of Japan) and Grants-in-Aid for Scientific Research (A) (No. 25246020 and No. 16H02333) from the Japan Society for the Promotion of Science (JSPS), and a Grant-in-Aid for Scientific Research on Innovative areas "Nano Spin Conversion Science" (No. 26103003) from the Ministry of Education, Culture, Sports, Science and Technology (MEXT). Y.F. acknowledges JSPS Research Fellowships for Young Scientists.

[1] X. Lou, C. Adelmann, S. A. Crooker, E. S. Garlid, J. Zhang, K. S. M. Reddy, S. D. Flexner, C. J. Palmstrøm, and P. A. Crowell, Nat. Phys. **3**, 197 (2007).
[2] P. Bruski, Y. Manzke, R. Farshchi, O. Brandt, J. Herfort, and M. Ramsteiner, Appl. Phys. Lett. **103**, 052406 (2013).
[3] G. Salis, A. Fuhrer, R. R. Schlittler, L. Gross, and S. F. Alvarado, Phys. Rev. B **81**, 205323 (2010).
[4] M. Ciorga, A. Einwanger, U. Wurstbauer, D. Schuh, W. Wegscheider, and D. Weiss, Phys. Rev. B **79**, 165321 (2009).
[5] T. Saito, N. Tezuka, M. Matsuura, and S. Sugimoto, Appl. Phys. Express **6**, 103006 (2013).
[6] I. Appelbaum, B. Huang, and D. J. Monsma, Nature (London) **447**, 295 (2007).
[7] O. M. J. van't Erve, A. T. Hanbicki, M. Holub, C. H. Li, C. Awo-Affouda, P. E. Thompson, and B. T. Jonker, Appl. Phys. Lett. **91**, 212109 (2007).
[8] T. Suzuki, T. Sasaki, T. Oikawa, M. Shiraishi, Y. Suzuki, and K. Noguchi, Appl. Phys. Express **4**, 023003 (2011).
[9] Y. Saito, T. Tanamoto, M. Ishikawa, H. Sugiyama, T. Inokuchi, K. Hamaya, and N. Tezuka, J. Appl. Phys. **115**, 17C514 (2014).
[10] B. Huang, D. J. Monsma, and I. Appelbaum, Phys. Rev. Lett. **99**, 177209 (2007).
[11] P. Li, J. Li, L. Qing, H. Dery, and I. Appelbaum, Phys. Rev. Lett. **111**, 257204 (2013).
[12] Y. Zhou, W. Han, L.-T. Chang, F. Xiu, M. Wang, M. Oehme, I. A. Fischer, J. Schulze, R. K. Kawakami, and K. L. Wang, Phys. Rev. B **84**, 125323 (2011).
[13] K. Kasahara, Y. Fujita, S. Yamada, K. Sawano, M. Miyao, and K. Hamaya, Appl. Phys. Express **7**, 033002 (2014).
[14] Y. Fujita, M. Yamada, S. Yamada, T. Kanashima, K. Sawano, and K. Hamaya, Phys. Rev. B **94**, 245302 (2016).
[15] S. A. Wolf, D. D. Awschalom, R. A. Buhrman, J. M. Daughton, S. von Molnár, M. L. Roukes, A. Y. Chtchelkanova, and D. M. Treger, Science **294**, 1488 (2001).
[16] I. Žutić, J. Fabian, and S. Das Sarma, Rev. Mod. Phys. **76**, 323 (2004).
[17] P. Li and H. Dery, Phys. Rev. Lett. **107**, 107203 (2011).
[18] Y. Song and H. Dery, Phys. Rev. B **86**, 085201 (2012).
[19] J. L. Cheng, M. W. Wu, and J. Fabian, Phys. Rev. Lett. **104**, 016601 (2010).
[20] J-M. Tang, B. T. Collins, and M. E. Flatté, Phys. Rev. B **85**, 045202 (2012).
[21] Y. Song, O. Chalaev, and H. Dery, Phys. Rev. Lett. **113**, 167201 (2014).
[22] L. Qing, J. Li, I. Appelbaum, and H. Dery, Phys. Rev. B **91**, 241405(R) (2015).
[23] M. Johnson and R. H. Silsbee, Phys. Rev. Lett. **55**, 1790 (1985).
[24] F. J. Jedema, H. B. Heersche, A. T. Filip, J. J. A. Baselmans, and B. J. van Wees, Nature (London) **416**, 713 (2002).
[25] T. Kimura and Y. Otani, J. Phys.: Condens. Matter **19**, 165216 (2007).
[26] Y. Saito, M. Ishikawa, H. Sugiyama, T. Inokuchi, K. Hamaya, and N. Tezuka, J. Appl. Phys. **117**, 17C707 (2015).
[27] S. Takahashi and S. Maekawa, Phys. Rev. B **67**, 052409 (2003).
[28] A. Fert and H. Jaffrès, Phys. Rev. B **64**, 184420 (2001).
[29] H. Jaffrès, J.-M. George, and A. Fert, Phys. Rev. B **82**, 140408(R) (2010).
[30] T. Yang, T. Kimura, and Y. Otani, Nat. Phys. **4**, 851 (2008).
[31] F. Casanova, A. Sharoni, M. Erekhinsky, and Ivan K. Schuller, Phys. Rev. B **79**, 184415 (2009).
[32] K. Hamaya, T. Kurokawa, S. Oki, S. Yamada, T. Kanashima, and T. Taniyama, Phys. Rev. B **94**, 140401(R) (2016).
[33] M. Kawano, K. Santo, M. Ikawa, S. Yamada, T. Kanashima, and K. Hamaya, Appl. Phys. Lett. **109**, 022406 (2016).
[34] T. Tahara, Y. Ando, M. Kameno, H. Koike, K. Tanaka, S. Miwa, Y. Suzuki, T. Sasaki, T. Oikawa, and M. Shiraishi, Phys. Rev. B **93**, 214406 (2016).
[35] See Supplemental Material at http://link.aps.org/supplemental/10.1103/PhysRevB.95.115302 for temperature-dependent D and τ_{Si}, estimated from electrical Hanle-effect measurements.
[36] T. Sasaki, T. Oikawa, T. Suzuki, M. Shiraishi, Y. Suzuki, and K. Noguchi, Appl. Phys. Lett. **96**, 122101 (2010).
[37] M. E. Flatté and J. M. Byers, Phys. Rev. Lett. **84**, 4220 (2000).
[38] O. Chalaev, Y. Song, and H. Dery, Phys. Rev. B **95**, 035204 (2017).
[39] We have confirmed a very small contribution of the $\frac{1}{\tau_{intra}}$ term in Eq. (2) when we used Eq. (13) in Ref. [17] in the analyses for our experiments.
[40] R. L. Aggarwal and A. K. Ramdas, Phys. Rev. **140**, A1246 (1965).
[41] T. G. Castner, Phys. Rev. **155**, 816 (1967).
[42] J. C. Hensel, H. Hasegawa, and M. Nakayama, Phys. Rev. **138**, A225 (1965).
[43] C. Herring and E. Vogt, Phys. Rev. **101**, 944 (1956).
[44] G. L. Pearson and J. Bardeen, Phys. Rev. **75**, 865 (1949).
[45] F. Mousty, P. Ostoja, and L. Passari, J. Appl. Phys. **45**, 4576 (1974).

[46] J. R. Prance, Z. Shi, C. B. Simmons, D. E. Savage, M. G. Lagally, L. R. Schreiber, L. M. K. Vandersypen, M. Friesen, R. Joynt, S. N. Coppersmith, and M. A. Eriksson, Phys. Rev. Lett. **108**, 046808 (2012).

[47] E. Kawakami, P. Scarlino, D. R. Ward, F. R. Braakman, D. E. Savage, M. G. Lagally, M. Friesen, S. N. Coppersmith, M. A. Eriksson, and L. M. K. Vandersypen, Nat. Nanotechnol. **9**, 666 (2014).

[48] K. Takeda, J. Kamioka, T. Otsuka, J. Yoneda, T. Nakajima, M. R. Delbecq, S. Amaha, G. Allison, T. Kodera, S. Oda, and S. Tarucha, Sci. Adv. **2**, e1600694 (2016).